Duality of diffusion dynamics in particle motion in soft-mode turbulence

Masaru Suzuki,[1,*] Hiroshi Sueto,[1] Yusaku Hosokawa,[1] Naoyuki Muramoto,[1] Takayuki Narumi,[2] Yoshiki Hidaka,[1,†] and Shoichi Kai[1]

[1]*Department of Applied Quantum Physics and Nuclear Engineering, Kyushu University, Fukuoka 819-0395, Japan*

[2]*Department of Mathematical Sciences, Kwansei Gakuin University, Sanda 669-1337, Japan*

(Received 5 February 2013; published 29 October 2013)

Nonthermal Brownian motion is investigated experimentally by injecting a particle into soft-mode turbulence (SMT), in the electroconvection of a nematic liquid crystal. It is clarified that the particle motion can be classified into two phases: fast motion, where particles move with the local convective flow, and slow motion, where they are carried by global slow pattern dynamics. We propose a simplified model to clarify the mechanism of the short-time and asymptotic behavior of diffusion. In our model, the correlation time is estimated as a function of a control parameter ε. The scaling of the SMT pattern correlation time, $\tau_d \sim \varepsilon^{-1}$, is estimated from the particle dynamics, which is consistent with a previous report observed from the Eulerian viewpoint. The origin of the non-Gaussian distribution of the displacement in the short-time regime is also discussed and an analytical curve is introduced that quantitatively agrees with the experimental data. Our results clearly illustrate the characteristics of diffusive motion in SMT, which are considerably different from the conventional Brownian motion.

DOI: 10.1103/PhysRevE.88.042147 PACS number(s): 05.40.−a, 05.45.−a, 47.52.+j

I. INTRODUCTION

The random motion driven by nonthermal fluctuations or chaotic flows [1–6] has been investigated in the context of nonlinear physics and statistical mechanics far from equilibrium. Among these phenomena, motion dynamics driven by soft-mode turbulence (SMT) in the electroconvection of a nematic liquid crystal is interesting because of the existence of hierarchical structures such as locally aligned convective rolls and a globally disordered structure [7,8]. Previous studies discussed the statistical-mechanical properties of the Brownian-like motion in SMT, such as anomalous behavior in the short time regime [4], the non-Gaussian distribution of velocity [5], and the application of the fluctuation theorem (FT) [6]. In these articles, although the asymptotic behavior of the finite-time diffusion coefficient was qualitatively associated with the local structure of SMT, the quantitative relation is still ambiguous.

In addition, the motion of an injected particle should provide a Lagrangian picture of SMT dynamics, which is expected to contain new information different from the SMT pattern dynamics itself. Supposing $\boldsymbol{V}(\boldsymbol{r},t)$ to be the flux vector field of SMT, the observation from the Eulerian viewpoint provides information about the pattern dynamics, $(\partial/\partial t)\boldsymbol{V}(\boldsymbol{r},t)$, while the local flux velocity $\boldsymbol{V}(\boldsymbol{r},t)$ itself is obtained by observing a particle that moves with the background flux. Thus, the particle motion should provide additional information that is not available from the Eulerian viewpoint, for example, the rotation speed of local convective rolls. Furthermore, as mentioned above, the particle motion is basically independent of relatively slow pattern dynamics, $(\partial/\partial t)\boldsymbol{V}(\boldsymbol{r},t)$; nevertheless, it may also contain some information about the pattern dynamics, because the motion of a particle with finite mass and finite size cannot be completely coherent with the local flow [9]. The particle is subjected to the pressure gradient of the SMT flow and may sometimes be trapped at black-lines [10] or domain boundaries of rolls [8]. Therefore, it can move with the pattern dynamics.

In this article, we introduce a new method of distinguishing the motion transported by the local flux from one carried by the pattern dynamics. Diffusive behaviors for both types are discussed using theoretical models, and typical time scales are estimated as a function of the SMT control parameter, ε.

II. EXPERIMENTAL SETUP

SMT is observed in the homeotropic alignment system of a nematic liquid crystal [8]. A nematic director aligned parallel to the z axis (the axis perpendicular to the electrode) tilts above the Fréedericksz point of the applied voltage, and the x-y projection of the director becomes a Nambu-Goldstone mode. Beyond the convective threshold voltage V_c, the long-range mode is disordered owing to the nonlinear coupling between the Nambu-Goldstone mode and the electroconvective mode, and SMT appears. Thus, the electroconvective mode is supercritical at the convection threshold in SMT [7].

To trace the motion of a particle in SMT, we injected small particles into a standard cell in homeotropic alignment (Fig. 1). The diameter and density of the particles (Micropearl) were $d = 6.48 \pm 0.17\ \mu$m and $\rho = 1.22 \times 10^3$ kg/m^3, respectively. Circular transparent electrodes of diameter 13.0 mm were used and the thickness of the cell was $97 \pm 3\ \mu$m.

The frequency of the applied voltage was set to be smaller than the Lifshitz frequency to perform the experiment in the oblique roll regime [11], since the fluctuations of the SMT are isotropic and sufficiently strong to drive the particles in this regime [12].

Images containing particles were sampled using a digital microscope (VHX-900, Keyence corporation) at a time interval of $\Delta t = 3$ s. This time interval is sufficiently small compared with the typical correlation time of the particle motion. Using the normalized voltage $\varepsilon = (V/V_c)^2 - 1$ as a control parameter, we observed the Brownian motion of particles at $\varepsilon = 0.05$, 0.075, 0.125, 0.150, and 0.6. The particle trajectory was traced for up to 600 s for each independent sample and statistical properties were measured by averaging at least 30 samples for each ε.

*suzuki@athena.ap.kyushu-u.ac.jp
†hidaka@ap.kyushu-u.ac.jp

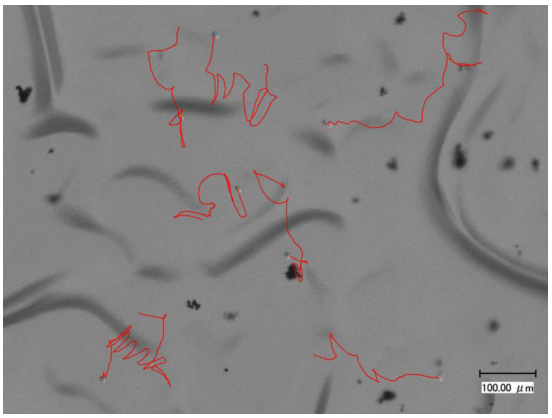

FIG. 1. (Color online) Particles in soft-mode turbulence. A solid curve shows the trajectory of each particle.

III. RESULTS

From the time series of the particle position $\boldsymbol{R}(t) = [x(t), y(t)]$, we measured the time-dependent diffusion coefficient,

$$D(\tau) = \frac{\langle |\boldsymbol{R}(t+\tau) - \boldsymbol{R}(t)|^2 \rangle}{2\tau}, \tag{1}$$

where $\langle \cdots \rangle$ denotes the sample and temporal average. As shown in Fig. 2, $D(\tau)$ sharply increases from 0, associated with ballistic motion, and then moderately increases until it reaches a constant value, i.e., that for normal diffusion, for each ε. To clarify the mechanism of this anomalous behavior, we carefully observed the particle trajectory and found that the particle motion can be classified into two phases: a phase with fast motion (named mode F) and a phase with slow motion (named mode S). We classified time series data $\{\boldsymbol{R}_i \equiv \boldsymbol{R}(t_i)\}$, $(t_{i+1} - t_i = \Delta t)$ into two phases as follows: defining the speed at $t = t_i$ to be $v_i \equiv |\boldsymbol{R}_{i+1} - \boldsymbol{R}_i|/\Delta t$, the ith data point is assumed to be in mode F if the average speed between $t_{i-2} \leqslant t \leqslant t_{i+2}$ is larger than the overall average speed and in mode S otherwise. The typical trajectories of both phases shown in Fig. 3 clearly illustrate that the characteristics of motion in both phases are markedly different. While oscillatory motion with a characteristic length is dominant in mode F, particles gradually change their direction of motion in mode S. Because switching between the two modes rarely occurs, we

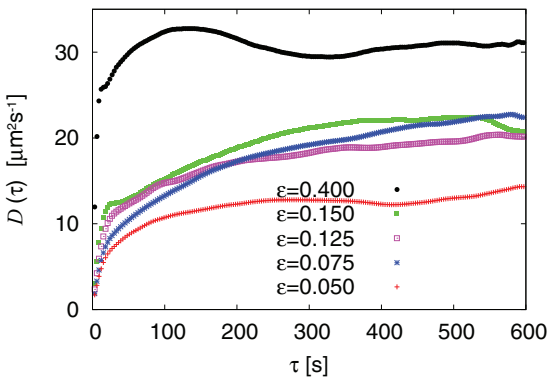

FIG. 2. (Color online) Time-dependent diffusion coefficient $D(\tau)$ for each value of ε.

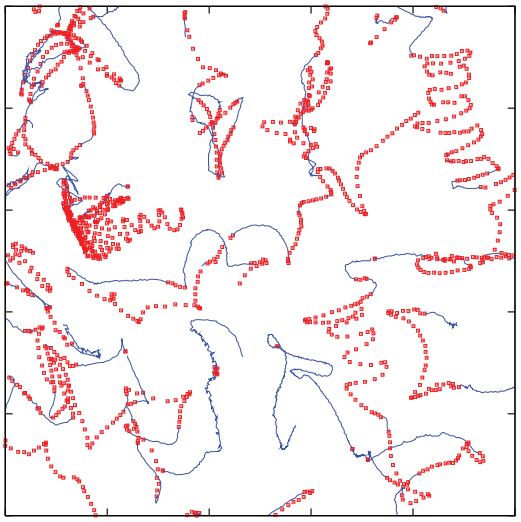

FIG. 3. (Color online) Plots with (red) squares show the trajectories of particle in mode F and solid (blue) curves show the trajectories of particles in mode S.

measured the time-dependent diffusion coefficients for modes F and S separately.

Mode S seems to appear when a particle fails to be transported by the convection and is carried by slow pattern dynamics. Its diffusion coefficient $D_s(\tau)$ monotonically increases with time as shown in Fig. 4. Thus, we simply assume the velocity autocorrelation in mode S to be

$$\langle \boldsymbol{v}(t) \cdot \boldsymbol{v}(t+\tau) \rangle = \langle v_s^2 \rangle \mathrm{e}^{-\tau/\tau_d}, \tag{2}$$

with a time constant of τ_d and the mean square velocity in mode S of $\langle v_s^2 \rangle$. Then, the diffusion coefficient is described as

$$D_s(\tau) = D_s^0[1 - (\tau_d/\tau)(1 - \mathrm{e}^{-\tau/\tau_d})], \tag{3}$$

with the asymptotic value of the diffusion coefficient $D_s^0 (\equiv \langle v_s^2 \rangle \tau_d)$. As shown in Fig. 4, experimental data are well fitted by Eq. (3) with the fitting parameters D_s^0 and τ_d. The correlation time τ_d decreases with increasing ε and is approximately scaled as $\tau_d = c\varepsilon^{-1}$ with a constant c (see Fig. 5). This scaling is similar to that of the SMT pattern correlation time [7,13], and the value $c = 3.0$ is of the same order as $c = 2.1$, obtained

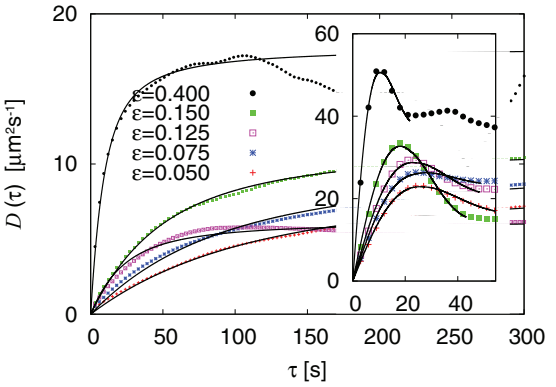

FIG. 4. (Color online) Time-dependent diffusion coefficient $D(\tau)$ for mode S. The points show experimental results and the solid curves are fitted using Eq. (3). The inset shows the diffusion coefficient for model F and fitting curves obtained using Eq. (4).

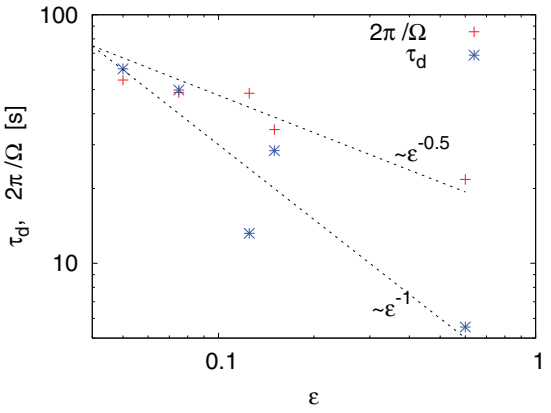

FIG. 5. (Color online) Correlation time for mode S, τ_d, and the cycle of the convective roll, $2\pi/\Omega$, estimated from the particle motion in mode F plotted against ε.

from pattern observation [13]. This fact suggests that during such a time scale, τ_d, the local structure of the SMT pattern exhibits regular motion (patch rotation, etc.), and thus a particle in mode S drifts without changing its direction of motion.

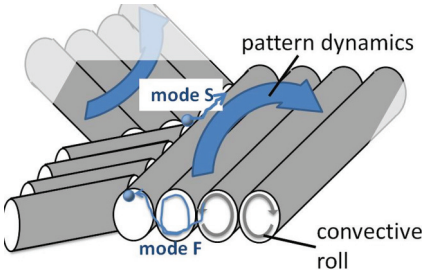

FIG. 6. (Color online) Schematic drawing of particle motion in SMT.

The oscillatory profile of the diffusion coefficient of mode F, shown in the inset of Fig. 4, suggests that this mode is associated with the motion carried by local convection. Such behavior for a relatively short time range can be approximated as the motion in one-dimensionally aligned convective rolls (see Fig. 6). We propose a model for mode F, where a particle is basically carried by a convective roll with diameter a and angular frequency Ω but has opportunities to hop to the next roll at the contacting edge with probability α. Under this assumption, the diffusion coefficient is written as

$$\frac{8\pi\tau}{a^2}D_f(\tau) = \begin{cases} \pi(1-\cos\Omega\tau)+\alpha(4\Omega\tau+2\Omega\tau\cos\Omega\tau-6\sin\Omega\tau) & (0<\tau\leqslant\pi/\Omega) \\ \pi+(2\alpha-1)\,[2\alpha(\pi-\Omega\tau)+\pi]\cos\Omega\tau+8\alpha(2\alpha-1)\sin\Omega\tau+8\alpha^2(\Omega\tau-\pi)+4\alpha\Omega\tau & (\pi/\Omega<\tau\leqslant 2\pi/\Omega) \end{cases}. \quad (4)$$

(see Appendix A). Although a deterministic model already exists for a similar system, the oscillating convection array [2,9], a stochastic model is used here for the hopping because the fluctuation of SMT is more chaotic. As shown in the inset of Fig. 4, the diffusion coefficient of mode F for each ε is well fitted using Eq. (4). The values of the fitting parameters a, Ω, and α are summarized in Table I. The estimated value of a is relatively small compared with the actual value (70–80 μm). This may be because the particles sometimes rotate in the inner region of the rolls. On the other hand, the estimated value of Ω should be more precise since this value sensitively depends on the sharp peak of the diffusion coefficient curve at $t=\pi/\Omega$. The rotation frequency approximately depends on ε as $\Omega\sim\sqrt{\varepsilon}$, as shown in Fig. 5. The diffusion coefficient D_f almost converge to a constant value after $t=2\pi/\Omega$ according to this model and the asymptotic value is $D_f\to a^2\alpha(\Omega/2\pi)/(1-\alpha)$ (see Appendix A). This value is more than three times larger than D_s^0. Therefore, the sharp increase in the total diffusion coefficient $D(\tau)$ at the initial stage is mainly due to the oscillatory motion in mode F, and the moderately increasing behavior in $D(\tau)$ in the later stage reflects motion in mode S.

TABLE I. Fitting coefficients for modes F and S.

ε	$2\pi/\Omega$ [s]	α	a [μm]	τ_d [s]	D_s^0 [μm^{2}s^{-1}]
0.050	54.6	0.29	43.9	60.6	8.84
0.075	48.7	0.37	43.0	49.8	10.1
0.125	48.3	0.30	46.3	13.2	6.28
0.150	34.5	0.18	48.2	28.4	11.4
0.600	21.7	0.30	41.1	5.54	17.8

Next, we observed the distribution of the particle displacement $l(\tau)=|\boldsymbol{R}(\tau)-\boldsymbol{R}(0)|$. In Fig. 7, the distribution $p(l,\tau)$, observed at $\varepsilon=0.05$, is shown after normalization by the standard deviation $\sigma(\tau)$ at each time interval τ, i.e., $\sigma(\tau)p(\tilde{l},\tau)$ is plotted against $\tilde{l}\equiv l/\sigma(\tau)$. As can be clearly seen, the distribution in the short-time interval has a stretched non-Gaussian tail that gradually converges to a Gaussian curve as the time interval increases.

As mentioned above, the motion in mode F should be dominant in the displacement distribution since its deviation is much larger than that in mode S. The local structure of a convective roll may induce such a stretched tail. Under the Markovian approximation for the hopping event, the probability of the number of hops in the time interval t is described by the Poisson distribution $\mathcal{P}_q(n,t)\equiv e^{-qt}(qt)^n/n!$ with a time constant q^{-1}. Under this simplification, the normalized distribution is written as

$$\sigma(\tau)p(\tilde{l},\tau) = \begin{cases} \frac{1}{2\pi}\exp(-\tilde{l}^2/2) & (\tilde{l}\lesssim\sqrt{q\tau}) \\ \sqrt{\sqrt{q\tau}/(2\pi\tilde{l})}\,e^{-q\tau}[e\sqrt{q\tau}/(2\tilde{l})]^{\sqrt{q\tau}\,\tilde{l}} & (\text{tail}) \end{cases} \quad (5)$$

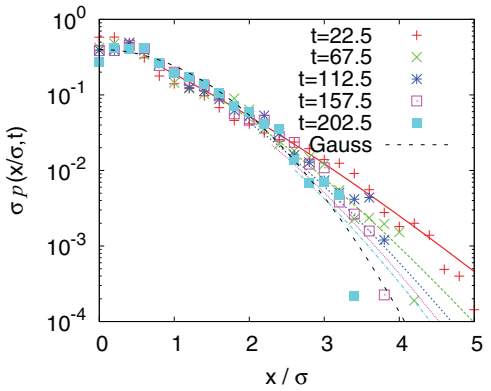

FIG. 7. (Color online) Normalized distribution of particle displacement at $\varepsilon = 0.05$. The non-Gaussian tail gradually converges to the Gaussian distribution (dashed curve). Other curves are drawn using the tail distribution in Eq. (5).

(see Appendix B). The variable q here is not a fitting parameter but is analytically associated with the parameters in Table I as $q = \alpha(\Omega/\pi)/(1-\alpha)$, because the diffusion coefficient of $D = qa^2/2$ under the assumption here should coincide with the asymptotic value of that in the model in Appendix A, $D_{\rm f} \to a^2\alpha(\Omega/2\pi)/(1-\alpha)$. As shown in Fig. 7, the tail distribution using the theoretical curves in Eq. (5) closely reproduces the experimental results without any free parameter.

IV. SUMMARY AND DISCUSSIONS

Features of the Brownian motion in SMT were observed in detail. It was found that the motion of the particle can be classified into two types. The first type (named mode F) mainly involves motion rotating with the local convective roll and sometimes hopping to the neighboring rolls. The hopping rate α and angular speed of the convection Ω were estimated using our model. The other type (named mode S) is motion moving with the slowly changing pattern dynamics of SMT. The correlation time of the velocity was estimated and its scaling, $\tau_d \sim \varepsilon^{-1}$, was obtained, which is consistent with the scaling of the pattern correlation time obtained from the Eulerian viewpoint. In Ref. [4], it was pointed out that the velocity distribution of a particle in SMT has a non-Gaussian form. Such a distribution may be observed as the result of superposition of these two modes. We also investigated the distribution of the particle displacement. It was clarified that the non-Gaussian tail in the short-time regime can be associated with the typical local structure (roll diameter) and the distribution of the hopping interval.

In preceding articles, we discussed how to describe the motion of a particle in SMT using a generalized version of the Langevin equation [4,6]. Thermal Brownian motion is accurately described by the Langevin equation,

$$m\frac{d}{dt}\boldsymbol{v}(t) = -\gamma\,\boldsymbol{v}(t) + \boldsymbol{\xi}(t) + \boldsymbol{F}, \tag{6}$$

with the friction constant γ, thermal noise $\boldsymbol{\xi}$, and external force $\boldsymbol{F}$. The velocity correlation time is associated with the friction constant as

$$\tau_v \equiv \frac{\int_0^\infty \langle \boldsymbol{v}(0)\cdot\boldsymbol{v}(t)\rangle dt}{\langle v(0)^2\rangle} = m/\gamma. \tag{7}$$

On the other hand, the Brownian motion of a particle in turbulent flux can be described as [9]

$$m\frac{d}{dt}\boldsymbol{v}(t) = -\gamma\{\boldsymbol{v}(t) - \boldsymbol{V}[\boldsymbol{r}(t),t]\} + \boldsymbol{F}. \tag{8}$$

In the case for a sufficiently large γ, the particle velocity is approximately

$$\boldsymbol{v}(t) \simeq \boldsymbol{V}[\boldsymbol{r}(t),t]; \tag{9}$$

thus, the macroscopic effective friction coefficient Γ, defined here to be

$$m/\Gamma \equiv \frac{\int_0^\infty \langle \boldsymbol{V}[\boldsymbol{r}(0),0]\cdot\boldsymbol{V}[\boldsymbol{r}(t),t]\rangle dt}{\langle \boldsymbol{V}(\boldsymbol{r}(0),0)^2\rangle} \tag{10}$$

is independent of the microscopic friction coefficient, γ, and is determined by the background flux. For example, the velocity correlation time for a particle in mode F is approximately the time required for the particle to lose its initial direction of motion, which is estimated as

$$m/\Gamma \simeq \sum_{n=1}^{\infty}(n\pi/\Omega)\alpha^n(1-\alpha) = (\pi/\Omega)\frac{\alpha}{1-\alpha}. \tag{11}$$

Since the mean square velocity v_0^2 is associated with the speed of the convective flow as

$$v_0 = a\Omega/2, \tag{12}$$

the diffusion constant is estimated to be

$$D_{\rm f} \simeq mv_0^2/\Gamma \simeq a^2\Omega\frac{\alpha}{1-\alpha}. \tag{13}$$

In the case with a constant external force, the average speed under the external force is, using Eq. (8) and assuming that $\langle \boldsymbol{V}\rangle = 0$,

$$\langle v\rangle = F/\gamma. \tag{14}$$

In the preceding article [6], the Brownian motion in SMT under an external force (the gravity, $F = mg$, with gravity constant g) was observed and the effective temperature T_E was measured assuming the Einstein relation

$$k_B T_E = \gamma D. \tag{15}$$

The estimated value of the effective temperature using the diffusion coefficient and $\gamma = mg/\langle v\rangle$ was $T_E \sim 10^6$ K, which is extremely large compared with the actual kinetic energy $m\langle v^2\rangle/k_B$. This large discrepancy is caused by the difference between the microscopic friction constant γ and the effective friction constant Γ. In a system with macroscopic turbulent flow, the average velocity as the response to an external force is determined by γ, while the amplitude of the deviation from the average velocity (diffusion) is determined by Γ. This fact clearly illustrates the difference between motion driven by the thermal fluctuation in a system in equilibrium and that driven by the macroscopic flow in a system far from equilibrium. Although Eqs. (6) and (8) have similar form, the characteristic of the term $\gamma\boldsymbol{V}$ is greatly different from that of noise term ξ. In

contrast to the Brownian motion in equilibrium system where the fluctuation-dissipation relation

$$\langle \xi(t)\xi(t')\rangle = 2m\langle v^2\rangle\gamma\delta(t-t') \tag{16}$$

is satisfied, there is no relation between γ and $\boldsymbol{V}$ in nonequilibrium systems, where turbulent flow is sustained by a steady energy supply.

In Ref. [6], the effective temperature was also estimated using FT [14]. Since we observed the displacement distribution for a large time interval is Gaussian, which would not change under a relatively small external force, i.e., $p(x,\tau) \sim \exp[-(x - F\tau/\gamma)^2/(4D\tau)]$, the distribution of power, $w \equiv Fx/\tau$, can be described as

$$p(w) \sim \exp\left[\frac{-(w-\langle w\rangle)^2}{4F^2D/\tau}\right], \tag{17}$$

with $\langle w\rangle = F^2/\gamma$. Thus, it is natural that the effective temperature estimated from FT, $(k_BT_{FT})^{-1} \equiv \ln[p(w)/p(-w)]/(w\tau) = (\gamma D)^{-1}$ was almost equivalent to that estimated from the Einstein relation, even in SMT.

One of the novel findings in this article is that as well as the local structure being obtained by observations in mode F, features of the pattern dynamics of SMT pattern dynamics are obtained via mode S. The timescale for which a particle remains in mode S should be controlled by changing the particle mass and/or diameter. Further details of SMT dynamics can be revealed by such treatment. The Brownian motion of a particle under a large external force, where the average drifting velocity is comparable with the fluctuating velocity and the diffusive motion is disturbed, will also be an interesting issue for further investigation.

ACKNOWLEDGMENT

This work was partially supported by KAKEHNI (Grants No. 20111003, No. 21340110, and No. 24540408).

APPENDIX A: DIFFUSION IN FLUCTUATING CONVECTION ARRAY

In a one-dimensional array of convective rolls, where the center position of the jth roll is at $x = ja$, a particle initially in the $j = 0$ roll with initial angle θ ($0 \leqslant \theta < \pi$) is assumed to rotate with the convective flow of each roll with angular frequency Ω and has an opportunity to hop to a neighboring roll at every $t = (\theta + n\pi)/\Omega$, ($n = 1,2,3,\ldots$). If the particle is in the jth roll at time t, the position x can be written as $x(t) = ja + (a/2)\cos(\theta - \Omega t + j\pi)$, regardless of how many times it undergoes hopping. In the time range $\Omega t < \theta$, the particle is deterministically in the initial roll ($j = 0$), and in the time range $\theta \leqslant \Omega t < \pi + \theta$, it is in the $j = 1$ roll with probability α or in the $j = 0$ roll with probability $1 - \alpha$. Thus, the expected value of the second-order moment of x averaged over the initial angle θ in the time range $0 \leqslant \Omega t < \pi$ is

$$\begin{aligned}\frac{4\pi}{a^2}\langle|x(t)-x(0)|^2\rangle &= \int_{\Omega t}^{\pi}[\cos(\theta-\Omega t)-\cos\theta]^2d\theta + (1-\alpha)\int_0^{\Omega t}[\cos(\theta-\Omega t)-\cos\theta]^2d\theta \\ &\quad + \alpha\int_0^{\Omega t}[2-\cos(\theta-\Omega t)-\cos\theta]^2d\theta \\ &= \int_0^{\pi}[\cos(\theta-\Omega t)-\cos\theta]^2d\theta + 4\alpha\int_0^{\Omega t}[\cos\theta\cos(\theta-\Omega t)-\cos\theta-\cos(\theta-\Omega t)+1]d\theta \\ &= \pi(1-\cos\Omega t)+\alpha(4\Omega t + 2\Omega t\cos\Omega t - 6\sin\Omega t). \end{aligned} \tag{A1}$$

In the same way, in the time range $\pi + \theta \leqslant \Omega t < 2\pi + \theta$, the particle is in the $j = 2$ roll with probability α^2, in $j = 1$ with $\alpha(1-\alpha)$, in $j = -1$ with probability $\alpha(1-\alpha)$, and in $j = 0$ with probability $(1-\alpha)^2$. Thus, the expected value of the second-order moment of x in the time range $\pi \leqslant \Omega t < 2\pi$ is

$$\begin{aligned}\frac{4\pi}{a^2}\langle|x(t)-x(0)|^2\rangle &= \int_{\Omega t-\pi}^{\pi}\{(1-\alpha)[\cos\theta-\cos(\theta-\Omega t)]^2+\alpha[\cos\theta+\cos(\theta-\Omega t)-2]^2\}d\theta \\ &\quad + \int_0^{\Omega t-\pi}\{(1-\alpha)^2[\cos\theta-\cos(\theta-\Omega t)]^2+\alpha(1-\alpha)[\cos\theta+\cos(\theta-\Omega t)-2]^2 \\ &\quad + \alpha(1-\alpha)[\cos\theta+\cos(\theta-\Omega t)+2]^2+\alpha^2[\cos\theta-\cos(\theta-\Omega t)-4]^2\}d\theta \\ &= \pi + (2\alpha-1)[2\alpha(\pi-\Omega t)+\pi]\cos\Omega t + 8\alpha(2\alpha-1)\sin\Omega t + 8\alpha^2(\Omega t-\pi)+4\alpha\Omega t. \end{aligned} \tag{A2}$$

To calculate the second-order moment at an arbitrary time, a discretized probability distribution $p_{n,j}$, which denotes the probability that the particle is in the jth roll in the time range $(n-1)\pi + \theta \leqslant \Omega t < n\pi + \theta$, is introduced. Following the above discussion, the recurrence formula of $p_{n,j}$ is described as

$$p_{n+1,i} = \begin{cases} \alpha p_{n,j-1} + (1-\alpha)p_{n,j} & [(n+j) \bmod 2 = 0] \\ \alpha p_{n,j+1} + (1-\alpha)p_{n,j} & [(n+j) \bmod 2 = 1] \end{cases}. \tag{A3}$$

Using $p_{n,j}$, the second-order moment of x at $t = n\pi/\Omega$ is written as

$$\begin{aligned}\frac{4\pi}{a^2}\langle|x(n\pi/\Omega)-x(0)|^2\rangle &= \int_0^\pi d\theta \sum_j [2j+(-1)^{n+j}\cos\theta-\cos\theta]^2 p_{j,n} \\ &= 4\int_0^\pi d\theta\left[\langle j^2\rangle_n - 2\cos\theta\langle j^1\rangle_n^{(1)} + \cos^2\theta\langle j^0\rangle_n^{(1)}\right] \\ &= 4\pi\langle j^2\rangle_n + 2\pi\langle j^0\rangle_n^{(1)}, \end{aligned} \tag{A4}$$

where

$$\begin{aligned}\langle j^k\rangle_n^{(b)} &\equiv \sum_i i^k p_{n,i}\delta_{(n+i)\bmod 2,b} \quad (b=0,1), \\ \langle j^k\rangle_n &\equiv \langle j^k\rangle_n^{(0)} + \langle j^k\rangle_n^{(1)}. \end{aligned} \tag{A5}$$

The kth-order moment of j, $\langle j^k\rangle$, is recursively calculated from Eq. (A3). The recurrence formula for the zeroth order,

$$\langle j^0\rangle_n^{(1)} = \alpha\langle j^0\rangle_{n-1}^{(1)} + (1-\alpha)\langle j^0\rangle_{n-1}^{(0)}, \tag{A6}$$

and vice versa for (b), leads to

$$\langle j^0\rangle_n = 1, \quad \text{and} \quad \langle j^0\rangle_n^- = -(2\alpha-1)^n, \tag{A7}$$

with $\langle j^k\rangle_n^- \equiv \langle j^k\rangle_n^{(1)} - \langle j^k\rangle_n^{(0)}$. Similarly,

$$\begin{aligned}\langle j^1\rangle_n^- &= (2\alpha-1)\langle j^1\rangle_{n-1}^- + \alpha\langle j^0\rangle_{n-1} \\ &= \frac{\alpha}{2(1-\alpha)}[1-(2\alpha-1)^n], \end{aligned} \tag{A8}$$

and for the second order,

$$\begin{aligned}\langle j^2\rangle_n &= \langle j^2\rangle_{n-1} + 2\alpha\langle j^1\rangle_{n-1}^- + \alpha\langle j^0\rangle_{n-1} \\ &= \frac{-\alpha^2}{2(1-\alpha)^2}[1-(2\alpha-1)^n] + \frac{\alpha}{1-\alpha}n. \end{aligned} \tag{A9}$$

Substituting these equations into Eq. (A4),

$$\begin{aligned}\frac{4\pi}{a^2}\langle|x(t)-x(0)|^2\rangle &= \frac{\pi(1-2\alpha-\alpha^2)}{(1-\alpha)^2}[1-(2\alpha-1)^{\Omega t/\pi}] \\ &\quad + \frac{4\pi\alpha}{1-\alpha}(\Omega t/\pi). \end{aligned} \tag{A10}$$

The value of this equation matches those of Eqs. (A1) and (A2) at $t = 0$, π/Ω, and $2\pi/\Omega$. The asymptotic value of the diffusion coefficient for this model is

$$\lim_{t\to\infty}\frac{\langle|x(t)-x(0)|^2\rangle}{2t} = \frac{a^2\Omega\alpha}{2\pi(1-\alpha)}. \tag{A11}$$

APPENDIX B: RANDOM WALK BASED ON POISSON PROCESS

Strictly speaking, the time a hopping event occurs and the time the next hopping event occurs are weakly correlated according to the model in Appendix A. However, a particle should gradually lose its initial phase due to the fluctuating dynamics of the flow, and at a larger time compared with the rotation period of rolls, Markovian approximation would be suitable for the hopping event. When it is assumed that the probability of the number of hops between convection rolls within the time interval t follows the Poisson process, $\mathcal{P}_q(n,t)$, the probability that a particle initially in the zeroth roll is in the jth roll at time t is

$$\begin{aligned}p_j(t) &= \sum_{k=0}^\infty \mathcal{P}_q(j+2k,t)\frac{{}_{j+2k}C_k}{2^{j+2k}} \\ &= \mathrm{e}^{-qt}(qt/2)^j\sum_{k=0}^\infty\frac{(qt/2)^{2k}}{(j+k)!k!}. \end{aligned} \tag{B1}$$

This distribution $p_j(t)$ satisfies the recurrence equation

$$\frac{p_{j+1}(t)-p_{j-1}(t)}{2} = -(j/qt)p_j(t). \tag{B2}$$

Comparing with the expansion of the Gaussian distribution

$$\begin{aligned}&\exp[-(x+\Delta x)^2/(2t)] \\ &\quad = \exp[-x^2/(2t)][1-(x/t)\Delta x + 2^{-1}(x/t)^2(\Delta x)^2+\cdots], \end{aligned} \tag{B3}$$

the distribution for small j ($|j| \ll qt$) can be approximated as

$$p_j(t) \simeq \frac{1}{\sqrt{2\pi qt}}\mathrm{e}^{-j^2/(2qt)}. \tag{B4}$$

On the other hand, for large j [$(qt)^2 \ll j$], the terms in the summation in Eq. (B1), $s_k \equiv \mathcal{P}_q(j,t)_{j+2k}C_k/2^{j+2k}$ satisfy

$$\frac{s_{k+1}}{s_k} = \frac{(qt/2)^2}{(j+k+1)(k+1)} \ll 1. \tag{B5}$$

Thus, taking only the leading term s_0, a Poisson-like tail appears in the displacement distribution as

$$\begin{aligned}p_j(t) &\simeq 2^{-j}\mathcal{P}_q(j,t) \\ &\simeq \frac{e^{-qt}}{\sqrt{2\pi j}}\left(\frac{eqt}{2j}\right)^j. \end{aligned} \tag{B6}$$

The second-order moment of j is

$$\begin{aligned}\langle j^2\rangle &= 2\sum_{j=0}^\infty j^2\sum_{k=0}^\infty \mathcal{P}_q(j+2k,t)\frac{{}_{j+2k}C_k}{2^{j+2k}} \\ &= 2\sum_{k=0}^\infty\sum_{j=2k}^\infty (j-2k)^2\mathcal{P}_q(j,t)\frac{{}_jC_k}{2^j} \\ &= \sum_{j=0}^\infty\sum_{k=0}^j (j-2k)^2\mathcal{P}_q(j,t)\frac{{}_jC_k}{2^j} \\ &= \sum_{j=0}^\infty j\mathcal{P}_q(j,t) = qt. \end{aligned} \tag{B7}$$

The roll index j can be associated with the continuous displacement as $l = aj$, and the standard deviation of l under this model is $\sigma(\tau) = a\sqrt{q\tau}$, thus, the normalized distribution, Eq. (5), is described by Eqs. (B4) and (B6).

[1] J.-P. Bouchaud and A. Georges, Phys. Rep. **195**, 127 (1990).
[2] T. H. Solomon and J. P. Gollub, Phys. Rev. A **38**, 6280 (1988).
[3] K. Ito and S. Miyazaki, Prog. Theor. Phys. **110**, 875 (2003).
[4] K. Tamura, Y. Yusuf, Y. Hidaka, and S. Kai, J. Phy. Soc. Jpn. **70**, 2805 (2001).
[5] K. Tamura, Y. Hidaka, Y. Yusuf, and S. Kai, Physica A **306**, 157 (2002).
[6] Y. Hidaka, Y. Hosokawa, N. Oikawa, K. Tamura, R. Anugraha, and S. Kai, Physica D **239**, 735 (2010).
[7] S. Kai, K. Hayashi, and Y. Hidaka, J. Phys. Chem. **100**, 19007 (1996).
[8] Y. Hidaka, K. Tamura, and S. Kai, Prog. Theor. Phys. Suppl. **161**, 1 (2006).
[9] H. Sakaguchi, Phys. Rev. E **65**, 067201 (2002).
[10] R. Anugraha, Y. Hidaka, T. Ueki, and S. Kai, Phys. Rev. E **80**, 041701 (2009).
[11] J.-H. Huh, Y. Hidaka, and S. Kai, J. Phys. Soc. Jpn. **68**, 1567 (1999).
[12] R. Anugraha, K. Tamura, Y. Hidaka, N. Oikawa, and S. Kai, Phys. Rev. Lett. **100**, 164503 (2008).
[13] F. Nugroho, T. Narumi, Y. Hidaka, J. Yoshitani, M. Suzuki, and S. Kai, Phys. Rev. E **85**, 030701(R) (2012).
[14] D. J. Evans, E. G. D. Cohen, and G. P. Morriss, Phys. Rev. Lett. **71**, 2401 (1993).